LU TP 94-7
May 1994

Heavy Quark Pair Multiplicity in e^+e^- Events

M.H. Seymour
Department of Theoretical Physics, University of Lund,
Sölvegatan 14A, S-22362 Lund, Sweden

Abstract

We calculate the multiplicity of heavy quark pairs in e^+e^- annihilation events, which arises from perturbative gluon splitting. Our result is exact to leading order in α_s, and resums large leading and next-to-leading logarithmic terms to all orders. We compare our results with Monte Carlo models, and find reasonable agreement with those based on the parton shower approach.

LU TP 94-7
May 1994

1 Introduction

Heavy quark production in e^+e^- annihilation is an important laboratory for a variety of physics processes. It is possible to separately measure the partial width of the Z boson to the heavy quark flavours[1], constraining the electroweak parameters of the Standard Model. Many features of the associated events are reliably predicted by perturbative QCD, and provide independent tests of the theory. In particular, differences between the properties of heavy quark and light quark events are generally under better theoretical control than the absolute properties of either[2,3]. Most of these studies are concerned with primary heavy quarks that are produced in the e^+e^- annihilation itself. However, another source arises from events in which the primary quarks emit gluons that split perturbatively into heavy quarks. Although interesting in their own right, such quarks are generally considered as backgrounds to the other studies. In this paper we calculate their average multiplicity in e^+e^- annihilation. This should be added to the electroweak partial width to predict the inclusive cross-section for heavy quark production.

There have been many theoretical studies of heavy quark production by gluon splitting in hadron collisions[4–6], where the multiplicity is high because the jets produced are predominatly gluon-initiated. It can be reliably calculated in perturbation theory because it is an infrared finite quantity, as the quark mass provides a natural infrared cutoff. However when calculating this multiplicity for jet scales well above the quark mass, large logarithmic terms arise at all orders in the perturbative expansion, spoiling its convergence. To make reliable predictions, these terms must be organised into an improved perturbation series that resums all large terms in the original series[7]. This was done to leading logarithmic accuracy in [5,6], resumming all terms of the form $\alpha_s^n \log^m,\ m = 2n-1$*.

In e^+e^- annihilation to hadrons, where the primary jets are exclusively quark-initiated, the rate is considerably suppressed by the requirement that the quark jets produce a gluon jet at a sufficient scale to produce the heavy quark pair. As shown in [6], the resummed results for quark jets are not reliable on their own at current energies, and need to be supplemented by the leading order matrix element. That is, in addition to including the logarithmic terms at all orders, the term proportional to α_s^2 should use the full expression for the exact dependence on the collision energy and quark mass. This was calculated in [8], but is not reliable without the resummed component. In this paper we recalculate it, and improve the resummed results of [6] to next-to-leading logarithmic accuracy.

Our result predicts an average multiplicity of bottom quark pairs in Z decays due to gluon splitting of 0.18%, which is about 0.8% of their total multiplicity, and is comparable to the current precision of combined results from the four LEP experiments[9]. The result for charm quark pairs is 1.3%, which is 8% of the total multiplicity.

The remainder of this paper is set out as follows: In sections 2 and 3 we give the leading order result, and discuss the accuracy of various approximate forms. In section 4 we calculate the heavy quark multiplicity to next-to-leading logarithmic accuracy, and show how to match this to the leading order expression. In section 5 we give some numerical results, and discuss their accuracy. In section 6 we compare our results with three of the most commonly used Monte Carlo models. Finally in section 7 we summarise the paper. An appendix contains additional details of the calculations discussed in sections 2–4.

*Note that our nomenclature is different from [6], where these terms were called next-to-leading. The $m = 2n$ terms that are leading in parton multiplicities are absent in the heavy quark case.

2 Leading Order

It is straightforward to calculate the leading order differential cross-section for the process

$$\gamma^* \longrightarrow \mathrm{q} + \bar{\mathrm{q}} + \mathrm{Q} + \bar{\mathrm{Q}}, \tag{1}$$

in the approximation where only the light quark, q, couples to the photon. We neglect interference with diagrams where the heavy quark, Q, couples to the photon and the light quark pair is produced by gluon splitting, which is extremely small (see the later discussion). It is a function of five non-trivial kinematic variables, and does not have a compact form.

If we integrate over the heavy quark momenta however, we arrive at a simple expression with two factorised pieces, corresponding to the emission of an off-shell gluon by the $\mathrm{q}\bar{\mathrm{q}}$ pair and the decay of this gluon,

$$\begin{aligned}\frac{1}{\sigma_0}d\sigma &= \frac{\alpha_s^2}{12\pi^2}C_F\, dx_1 dx_2 \frac{dx_g^2}{x_g^2}\sqrt{1-x^2/x_g^2}\left(1+\frac{x^2}{2x_g^2}\right) \\ &\quad \left\{\frac{x_1^2+x_2^2}{(1-x_1)(1-x_2)} - x_g^2\frac{2(1+x_1+x_2)(1-x_1)(1-x_2)-(2-x_1-x_2)^2}{(1-x_1)^2(1-x_2)^2}\right. \\ &\quad \left. +x_g^4\frac{2}{(1-x_1)(1-x_2)}\right\},\end{aligned} \tag{2}$$

where $x_g^2 = m_g^2/s$, $x^2 = 4m_Q^2/s$, and $x_{1,2,3}$ are the energy fractions of the light quark, antiquark and massive gluon respectively. The curly bracket corresponds to the production part, which reduces to the well-known gluon emission formula when the mass is small. In general one would only expect the cross-section to factorise in this limit. However, after boosting to the gluon's rest-frame, the rest of the system can be described by just two angles, and the dependence on each is killed by one of the angular integrations of the heavy quark pair. Thus the gluon decay depends only on its mass, and the cross-section completely factorises. By normalising the cross-section to σ_0, the total cross-section for

$$\gamma^* \longrightarrow \mathrm{q} + \bar{\mathrm{q}}, \tag{3}$$

and averaging over the Euler angles, it becomes independent of the identity of the vector boson, and so is equally valid at the Z peak.

To integrate this expression to obtain the total cross-section, it is convenient to use the kinematic variables introduced in the dipole model, $k_\perp^2 = (1-x_1)(1-x_2)$ and $y = \frac{1}{2}\log(1-x_1)/(1-x_2)$,

$$\begin{aligned}\frac{1}{\sigma_0}d\sigma &= \frac{\alpha_s^2}{12\pi^2}C_F\, dy \frac{dk_\perp^2}{k_\perp^2}\frac{dx_g^2}{x_g^2}\sqrt{1-x^2/x_g^2}\left(1+\frac{x^2}{2x_g^2}\right) \\ &\quad \left\{\left(2-4k_\perp\cosh y+2k_\perp^2\cosh 2y\right)+x_g^2\left(4-2\cosh 2y-4k_\perp\cosh y\right)+x_g^4\left(2\right)\right\}.\end{aligned} \tag{4}$$

The kinematic limits are

$$\begin{array}{rcccl} x_g &<& k_\perp &<& (x_g^2+1)/2\cosh y, \\ \log x_g &<& y &<& -\log x_g, \\ x^2 &<& x_g^2 &<& 1. \end{array} \tag{5}$$

Two of these dimensions can be integrated analytically to leave a single integral, which must be performed numerically. Interested readers can find details in the appendix. The result for the average multiplicity of heavy quark pairs in e^+e^- annihilation is

$$\begin{aligned}\mathcal{N} \;\equiv\; \frac{1}{\sigma_0}\sigma \;=\; & \left(\frac{\alpha_s}{4\pi}\right)^2 \frac{4}{3} C_F \int_{x^2}^{1} dz \Biggl\{ \\ & \frac{1}{z}\sqrt{1-\frac{x^2}{z}}\left(1+\frac{x^2}{2z}\right)\left[(1+z)^2\log^2 z + 5 - 5z^2 + (3+4z+3z^2)\log z\right] \\ & + \frac{\log z}{1+z}\left[\sqrt{1-\frac{x^2}{z}}\left(-\frac{20}{3} - 8x^2 - \frac{4x^2}{3z} + 8z + x^2 z + 2z^2\right)\right. \\ & \left.\left. - (8-3x^4)\log x + (8-3x^4)\log\left(\sqrt{z}+\sqrt{z-x^2}\right)\right]\right\}. \qquad (6)\end{aligned}$$

We give numerical results of this integral in a later section.

In the limit of small x it becomes approximately

$$\begin{aligned}\mathcal{N} \;\approx\; & \left(\frac{\alpha_s}{4\pi}\right)^2 C_F \frac{4}{3}\left\{-\frac{1}{3}\log^3 x^2 - \left(\frac{19}{6} - \log 4\right)\log^2 x^2\right. \\ & \left. - \left(\frac{146}{9} - \frac{2}{3}\pi^2 - \frac{19}{3}\log 4 + \log^2 4\right)\log x^2 + 1.711\ldots\right\} \qquad (7)\end{aligned}$$

where the neglected terms are zero in the $x \to 0$ limit. If instead of the quark mass, x, we define an effective mass,

$$x^* \equiv \tfrac{1}{2} e^{5/6} x \approx 1.15x, \qquad (8)$$

this takes on a much simpler form,

$$\mathcal{N} \approx \left(\frac{\alpha_s}{4\pi}\right)^2 C_F \frac{4}{3}\left\{-\frac{1}{3}\log^3 x^{*2} - \frac{3}{2}\log^2 x^{*2} - \left(\frac{76}{9} - \frac{2}{3}\pi^2\right)\log x^{*2} + 2.359\ldots\right\}. \qquad (9)$$

It is interesting that this is exactly the same effective mass as that which appears in attempts to simplify two-loop calculations by appropriate modifications to one-loop results[10]. We discuss this in more detail later.

3 Approximations

In all-order calculational schemes, such as NLLA evolution and Monte Carlo models, various approximations are made to allow sequential splittings to factorise. It is useful to apply the same approximations to the fixed-order result, to gauge their accuracy.

The first approximation we consider is to take the limit of small gluon mass in the gluon emission part (the curly bracket of (2)), while retaining the full mass dependence of the gluon decay. We call this the full colour dipole model (fCDM) approximation. We also take the small-mass limit of the phase-space limits,

$$\begin{array}{rcccl} x_g & < & k_\perp & < & 1/2\cosh y, \\ -\cosh^{-1} 1/2x_g & < & y & < & \cosh^{-1} 1/2x_g, \\ x^2 & < & x_g^2 & < & 1/4. \end{array} \qquad (10)$$

The resulting integral form is given in the appendix. In the limit of small x it is approximately

$$\mathcal{N}_{\mathrm{fCDM}} \approx \left(\frac{\alpha_s}{4\pi}\right)^2 C_F\,\frac{4}{3}\left\{-\frac{1}{3}\log^3 x^{*2} - \frac{3}{2}\log^2 x^{*2} - \left(\frac{85}{9} - \frac{2}{3}\pi^2\right)\log x^{*2} - 2.545\ldots\right\}. \quad (11)$$

This approximation correctly reproduces the first two logarithms, but not the sub-dominant one.

We next consider the full parton shower (fDGLAP) approximation. This takes both the limit of small gluon mass and the collinear limit of the gluon emission part, and extrapolates that to all angles. Since this also reproduces the soft limit and its first correction, it is a better approximation in general than it sounds. This results in only a minor change relative to the fCDM approximation,

$$x_1^2 + x_2^2 \longmapsto 1 + (1 - x_3)^2 \quad (12)$$

in the numerator of the cross-section, with the same phase-space limits. The integral is again given in the appendix, and has the small-x limit

$$\mathcal{N}_{\mathrm{fDGLAP}} \approx \left(\frac{\alpha_s}{4\pi}\right)^2 C_F\,\frac{4}{3}\left\{-\frac{1}{3}\log^3 x^{*2} - \frac{3}{2}\log^2 x^{*2} - \left(\frac{94}{9} - \frac{2}{3}\pi^2\right)\log x^{*2} - 5.545\ldots\right\}. \quad (13)$$

Again, this agrees with the full result for the first two logarithms, but not the sub-dominant one.

We next consider also dropping mass effects in the gluon decay. We call these the leading (lCDM and lDGLAP) approximations. In the limit of small x these are approximately

$$\mathcal{N}_{\mathrm{lCDM}} \approx \left(\frac{\alpha_s}{4\pi}\right)^2 C_F\,\frac{4}{3}\left\{-\frac{1}{3}\log^3 x^2 - \frac{3}{2}\log^2 x^2 - \left(6 - \frac{1}{3}\pi^2\right)\log x^2 - 2.257\ldots\right\}, \quad (14)$$

$$\mathcal{N}_{\mathrm{lDGLAP}} \approx \left(\frac{\alpha_s}{4\pi}\right)^2 C_F\,\frac{4}{3}\left\{-\frac{1}{3}\log^3 x^2 - \frac{3}{2}\log^2 x^2 - \left(7 - \frac{1}{3}\pi^2\right)\log x^2 - 5.257\ldots\right\}. \quad (15)$$

The effective mass has not appeared, but the $\alpha_s^2 \log^2$ terms are otherwise correct.

We conclude that from the theoretical viewpoint, the CDM and DGLAP approximations are equally good—both get the leading two logarithms right, but not the sub-leading ones. However, the discrepancy in the next-to-next-to-leading logarithm is less than half the size in the CDM compared to DGLAP, so we would expect it to be numerically a better approximation.

On the other hand, in both cases taking the leading part of the gluon decay results in an incorrect next-to-leading logarithm, so is theoretically unattractive. However, this can be remedied as a calculational prescription, by using the leading result, but with the quark mass, m_Q, replaced by $m_Q^* = \frac{1}{2}\exp(5/6)m$.

This statement remains true at all orders, as can be seen by comparing the integral over the gluon mass in the leading approximation,

$$\lim_{x^2\to 0}\int_{x^2}^{a}\frac{dz}{z}\log^{n-1} z = -\frac{1}{n}\log^n x^2, \quad (16)$$

with the equivalent with the full mass dependence,

$$\lim_{x^2\to 0}\int_{x^2}^{a}\frac{dz}{z}\sqrt{1-\frac{x^2}{z}}\left(1+\frac{x^2}{2z}\right)\log^{n-1} z = -\frac{1}{n}\log^n x^{*2} + \mathcal{O}(\log^{n-2}). \quad (17)$$

Thus we can make a next-to-leading logarithmic prediction for the multiplicity of heavy quark pairs in any process at arbitrary order in α_s, simply by calculating it in the leading approximation, and then replacing m_Q by m_Q^*. This is just as expected from [10] where the effect of virtual heavy quark loops on the running coupling is considered in a similar way.

4 Resummed Calculation

The resummed results for the multiplicity of gluons in a quark or gluon were derived to next-to-leading logarithmic accuracy in [11]. Results were also given for the multiplicity of massless quarks but, as discussed in [6], these are only accurate to leading logarithmic order, and give an inaccurate prediction for the preexponential factor.

Explicit integration of the next-to-leading multiplicity of gluons with the full gluon splitting kernel will, however, give the correct next-to-leading multiplicity of heavy quark pairs. Since the appropriate integrals are not analytically tractable, we use our experience from the previous section to simplify the problem, by first using the leading kernel, and then replacing the heavy quark mass by the effective mass.

We use the same notation as [6], and do not repeat the definitions here. The relevant integrals are (57–59) of [6], which we improve to next-to-leading logarithmic accuracy in the appendix,

$$\begin{aligned}
\int_{z_0}^{z_1} \frac{dz}{z}\mathcal{N}^+(z,z_1) &= \widetilde{\mathcal{N}}_1(z_0,z_1) - \frac{2}{z_0^2}\left(1 - B\left(1-\frac{z_0}{z_1}\right)\right)\mathcal{N}^+(z_0,z_1) + \frac{2}{z_1^2} + \ldots, && (18)\\
\int_{z_0}^{z_1} \frac{dz}{z}\mathcal{N}^-(z,z_1) &= \frac{3}{8}\frac{C_A}{C_F}\frac{b}{n_f}\left(1 - \mathcal{N}^-(z,z_1)\right), && (19)\\
\int_{z_0}^{z_1} \frac{dz}{z}\widetilde{\mathcal{N}}(z,z_1) &= \frac{1}{z_0 z_1}\mathcal{N}^+(z_0,z_1) - \frac{1}{z_1^2} + \ldots, && (20)
\end{aligned}$$

where $\widetilde{\mathcal{N}}_k$ is defined to be identical to $\widetilde{\mathcal{N}}$, but with B replaced by $B-k$. Thus we obtain the next-to-leading order expressions for the multiplicity of quarks in quark and gluon jets,

$$\begin{aligned}
\mathcal{N}_q^q(Q_0,Q) &= \mathcal{N}^-(z_0,z_1) + C\widetilde{\mathcal{N}}_1(z_0,z_1)\\
&\quad -C\frac{1}{z_1^2}(2B-2-6C_A/b-C) - C\left(\frac{1}{z_0 z_1}(6C_A/b+C) - \frac{2}{z_0^2}(B-1)\right)\mathcal{N}^+(z_0,z_1), \qquad (21)\\
\mathcal{N}_g^q(Q_0,Q) &= \frac{8}{3}\frac{n_f}{b}\Bigg\{\widetilde{\mathcal{N}}_1(z_0,z_1)\\
&\quad + \left(\frac{2}{z_0^2}(B-1) - \frac{1}{z_0 z_1}(2B+C)\right)\mathcal{N}^+(z_0,z_1) + \frac{1}{z_1^2}(C+2)\Bigg\} \qquad (22)
\end{aligned}$$

where $C = \frac{8C_F n_f}{3C_A b}$, and everything else is as in [6]. The more accurate treatment has fixed the order of $\widetilde{\mathcal{N}}$, and added terms proportional to $1/z^2$.

We obtain the multiplicity of heavy quark pairs in e^+e^- annihilation to light quarks, as

$$\mathcal{N} = 2\left(\mathcal{N}_q^q(Q_0,Q) - 1\right)/2n_f, \qquad (23)$$

with

$$\begin{aligned}
Q_0 &= 2m_Q^* = m_Q e^{5/6}, && (24)\\
Q &= \sqrt{s}. && (25)
\end{aligned}$$

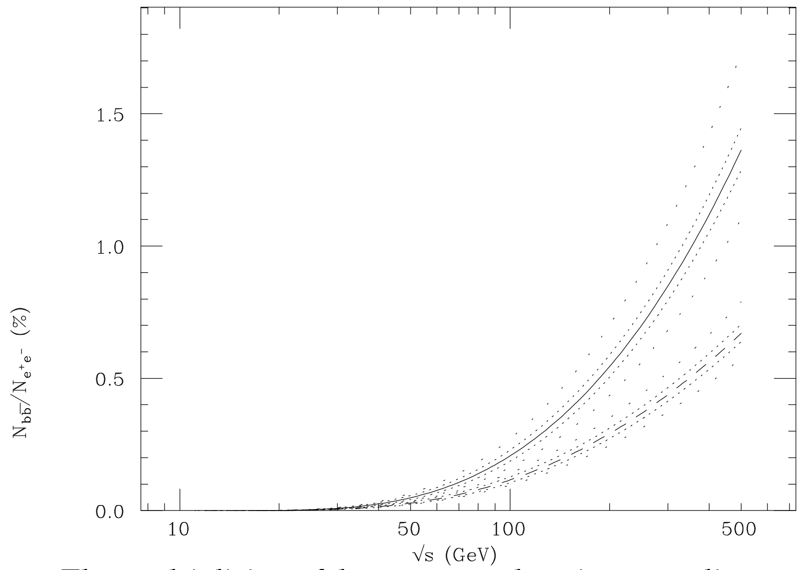

Figure 1: The multiplicity of bottom quark pairs according to the leading-order matrix element (dashed) and matched resummed result (solid). Also shown are the results of varying the quark mass by 5% (fine-dotted) and Λ by a factor of 2 (dotted).

This has threshold expansion

$$\mathcal{N} \;=\; \left(\frac{\alpha_s}{4\pi}\right)^2 C_F \left\{\frac{32}{9}L^3 - 8L^2 + L\frac{2}{27C_A^4}\Big(99C_A^4 + 54C_A^3 n_f - 28C_A^2 C_F n_f \right. \\ \left. -32C_A^2 n_f^2 + 88C_A C_F n_f^2 - 64C_F^2 n_f^2\Big)\right\} + \mathcal{O}(\alpha_s^3), \qquad (26)$$

where $L = \log Q/Q_0$. Unlike the first two terms, the coefficient of $\alpha_s^2 L$ is not the correct one, since it is a next-to-next-to-leading term. Nevertheless, the value quoted should be subtracted from the resummed result to match it with the fixed-order result. This matching is done simply by adding the two results together, and subtracting the terms they have in common, ie. Eq. (26).

We find that very close to threshold for five or more flavours, the matched expression becomes negative, which is of course unphysical. One might consider a more sophisticated matching procedure as used in event shapes, or as in [6], but since the result for b quarks is already well-behaved by $\sqrt{s} = 20$ GeV, where it is certainly still too small to be observed, we do not consider it necessary.

5 Numerical Results

In Fig. 1 we show the multiplicity of bottom quark pairs in e^+e^- annihilation to light quarks, as a function of the centre-of-mass energy. We set $m_b = 5$ GeV, and $\Lambda = 150$ MeV, although it should be noted that this is not relatable to $\Lambda_{\overline{\mathrm{MS}}}$, since the leading scheme-dependent terms are not treated in either the fixed-order or resummed part. The resummation is clearly important whenever the multiplicity is large enough to be observed. Also shown is the result of varying Λ by a factor of two, which makes a 25% difference, roughly constant with energy, and the bottom quark mass by 5%, which makes a 10% difference at the Z mass, reducing with energy. Table 1 lists the predictions for e^+e^- annihilation at the

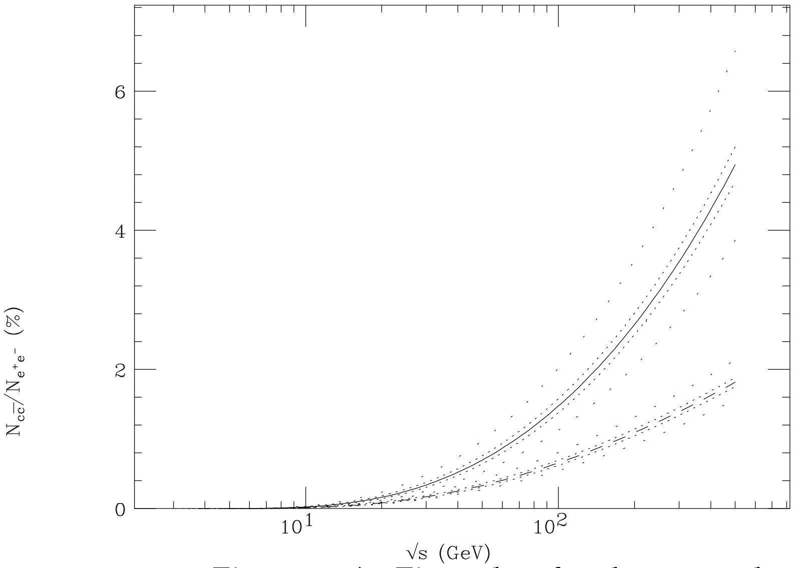

Figure 2: As Fig. 1, but for charm quark pairs.

Z mass for all the different methods we discuss. Note that the leading order results are in good agreement with [8]†, but that these are much smaller than the full results.

In Fig. 2 we show the equivalent graph for charm quark pairs, with $m_c = 1.5$ GeV. As one would expect, the resummation is more important. From here on, we concentrate on bottom quark pairs, but our comments are equally valid for charm quark pairs.

In Fig. 3 we show the multiplicity of bottom quark pairs at leading order, using the various approximations discussed earlier. As anticipated, CDM is better than DGLAP, and full is better than leading. The fCDM approximation is almost exact over most of the

†In fact the method of [8] only keeps track of terms that are non-vanishing in the $m_q^2/s \to 0$ limit, i.e. it is equivalent to our Eq. (7). For charm quarks, this difference is very small, but for bottom quarks (7) overestimates (6) by more than 10%. Using the approximation of (7) and their value of $\alpha_s = 0.12$, we obtain exact agreement with [8].

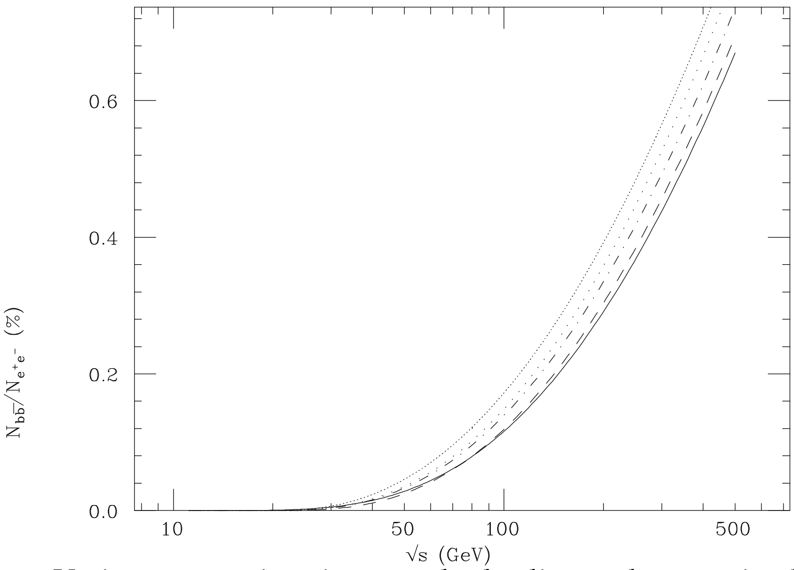

Figure 3: Various approximations to the leading order matrix-element result for the multiplicity of bottom quark pairs: exact (solid), fCDM (dashed), fDGLAP (dot-dashed), lCDM (dotted), lDGLAP (fine-dotted).

energy range considered, although it becomes too low near threshold.

One can get a rough idea of the accuracy of the predictions from the variations shown in Figs. 1 and 2. In principle, the Λ value in NLLA calculations is completely unknown and process-specific, and so there is no reason to confine it to any particular range. However, one might hope that since the multiplicity of heavy quarks is completely determined by the multiplicity of gluons, that it would agree with the fit to NLLA multiplicity distributions, $\Lambda = 150$ MeV, essentially absorbing the common next-to-next-to-leading effects into the fitted value of Λ. If one takes this approach, then the factor of two variation shown is certainly an over-estimate of the uncertainty.

When dealing with quarks, one is never completely free from confinement effects, even for energy scales far above their mass. These effects can be absorbed as an effective quark mass (which should not be confused with the effective mass defined earlier, which is purely perturbative, and arises even in QED). Without a more detailed treatment of these effects, the best one can manage is to vary the quark mass between the current mass ~ 4.75 GeV, and the meson mass ~ 5.25 GeV, as shown in Fig. 1.

Another uncertainty comes from the fact that the calculation starts from light quarks, while e^+e^- annihilation provides an admixture of quark flavours, including some charm and bottom quarks. In the following section we estimate this from Monte Carlo, which results in a suppression of up to 10%.

We can estimate the neglected contribution from interference with diagrams where the heavy quark pair emits a gluon that splits to the light quark pair, by using a result from [12]. At leading order in α_s, the interference is zero for the vector current because the quark loops each have three vector couplings. The axial terms for degenerate u- and d-type quarks exactly cancel, leaving only terms where the 'light' and 'heavy' quarks are both bottom quarks. These are infrared finite, so can be calculated in neglect of the quark mass. The result is[12]

$$\frac{\sigma_I}{\sigma_0} = \frac{1}{3}\left(\frac{\alpha_s}{\pi}\right)^2 I_4 \frac{a_b^2}{\sum_i (v_i^2 + a_i^2)}, \tag{27}$$

where $I_4 \approx 0.460$ and v_i, a_i are the vector and axial couplings of quark i, which give $a_b^2/\sum_i(v_i^2 + a_i^2) \approx 0.148$. At the Z mass, this corresponds to less than 1/500th of our result. The first non-zero term for the vector current would be comparable to this because although it is suppressed by α_s, it is not restricted to the bottom quark coupling.

The most difficult uncertainty to estimate is that due to neglected terms in the perturbation series. The variation with Λ gives some indication of its size, since at this order it is equivalent to varying the factorisation scale, and the first neglected term should cancel this dependence. In the next section we estimate one neglected contribution that enters at next-to-next-to-leading logarithmic accuracy, corrections due to energy conservation, which one might naïvely expect to be the largest neglected term. We find that at the Z mass it makes a difference of 15%, slowly increasing with energy. Again, the optimistic view would be that the fitting of Λ to multiplicity data means that these effects are included to a large extent, and varying Λ within the range allowed by the fit should give the full theoretical uncertainty. Nevertheless we remain more conservative, in quoting the largest uncertainty we have considered, 25%, as the overall theoretical uncertainty. For charm quarks this is 30%. Note that the main neglected effects reduce the prediction, so we expect our results to give a reasonable upper bound on the actual multiplicity.

6 Monte Carlo Models

Although Monte Carlo models are less accurate than explicit calculations, they provide a detailed description of the hadron-level final state, on an event-by-event basis. This means that it is often only possible, or convenient, to compare experimental results with the model predictions. It is therefore important to test the models using analytical results whenever possible, to check that they are accurate representations of the underlying theory.

The three most commonly used models, HERWIG[13], JETSET[14] and ARIADNE[15], all provide descriptions of the parton cascade process that are accurate to leading logarithmic order, together with matching to the first-order result for the production of a hard gluon. In the light of our analytical results, one might expect them to be accurate to around 20%.

One way in which Monte Carlo results are more reliable than resummed calculations is that they include suppression due to competition for phase-space between different types of emission. Namely, between gluon emission and gluon splitting. This is formally a next-to-next-to-leading effect, and is thus neglected in next-to-leading order analytical calculations, but it can have a radical effect for certain observables[16]. In a time-ordered picture, the physical origin of this suppression is clear—soft gluons carry away energy, and so emission from the light quark and massive gluon prior to the gluon splitting reduces its energy, and thus the phase-space available for the splitting. At next-to-leading order soft gluons exactly cancel the Sudakov form factor, and so have no influence on subsequent emissions.

However, the definition of 'time' in which events are ordered is the area in which the models differ most. If there were only one type of emission this would not be important, and all the models would give the same cross-section, but it is obviously an important difference for competition effects. In HERWIG, which uses decreasing opening angle as increasing time, many soft gluons are emitted on average before a gluon splitting at a given virtuality. In ARIADNE, which uses decreasing transverse momentum, all previous emission must be harder than the decay of the gluon, so there is rarely any earlier emission. Therefore all else being equal (which of course it never is), one would expect ARIADNE to approximate the next-to-leading order curve, with HERWIG somewhat below it. JETSET, which uses virtuality as ordering variable would lie between the two. This was proposed in [17] as a crucial test to differentiate between the models. We estimate its size shortly.

In Fig. 4, we show the model results in comparison with the analytical one. We leave all parameters at their default values, and use HERWIG5.7, JETSET7.3 and a preliminary version of ARIADNE that fixes a bug found since the last public version, 4.04[18]. We only generate light quark events, to allow a direct comparison with the analytical result (see below). The statistical errors for JETSET and ARIADNE are not negligible, because many events must be generated to count the small fraction of them that contain heavy quarks. In HERWIG, it is possible to directly generate such events[6][‡], and so the statistics are far better. JETSET agrees well with the analytical result, while HERWIG is a little high at the Z mass, falling into good agreement at higher energy. However, ARIADNE lies far above the analytical result.

In Fig. 5, we show the equivalent for charm quark pairs, where the agreement is not so good. This is because of the charm quark masses used: In JETSET the default is 1.35 GeV and the full expression for gluon decay is used, while in HERWIG the default is 1.8 GeV, onto which is added an infrared cutoff of 0.5 GeV and the leading expression for gluon

[‡]This requires a package of additional routines, available upon request from the author.

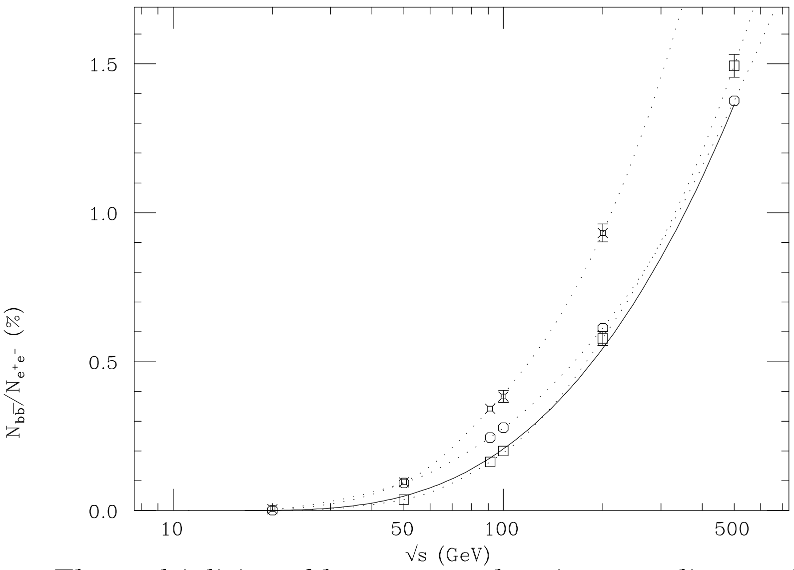

Figure 4: The multiplicity of bottom quark pairs according to the analytical result, using $\Lambda = 150$ MeV (solid). Points are from HERWIG (circles), JETSET (squares), and ARIADNE (crosses). Monte Carlo errors are shown where they are larger than the plotting symbols.

decay is used. Thus by setting $m_c = 1.5$ GeV in JETSET and $1.5 \times 1.15 - 0.5 = 1.2$ GeV in HERWIG, one would expect better agreement (the default values for m_b, 5 GeV and 5.2 GeV respectively, already agree with the bottom quark mass used in our calculation). This improves the agreement to a similar level as for bottom quarks. We have not checked what effect it has on the predictions for other features of e^+e^- events.

It seems that the over-estimate of the multiplicity predicted by ARIADNE is too large to be explained by competition effects. Indeed, all else being equal, such effects can only decrease the model predictions below the analytical one, not increase them. To confirm this however, it would be useful to be able to estimate the size of the competition effects.

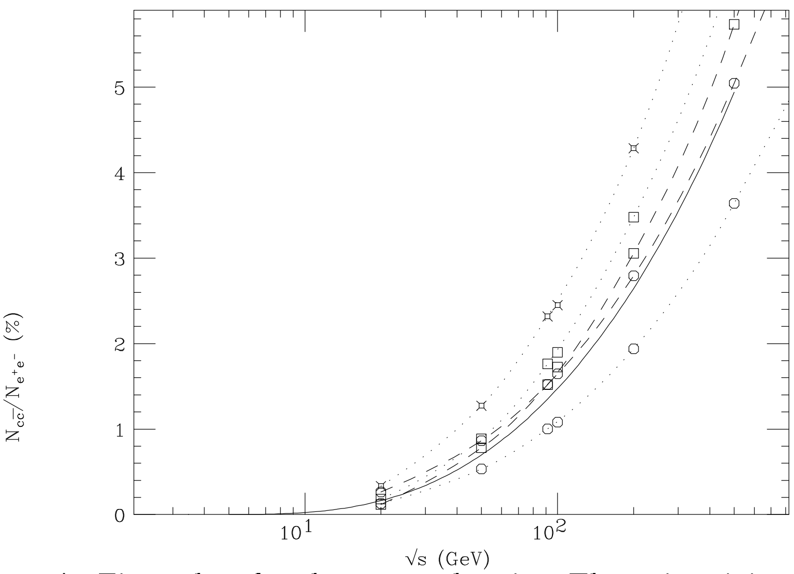

Figure 5: As Fig. 4, but for charm quark pairs. The points joined by dotted curves use the default values of the charm quark mass, while those joined by dashed curves use modified values.

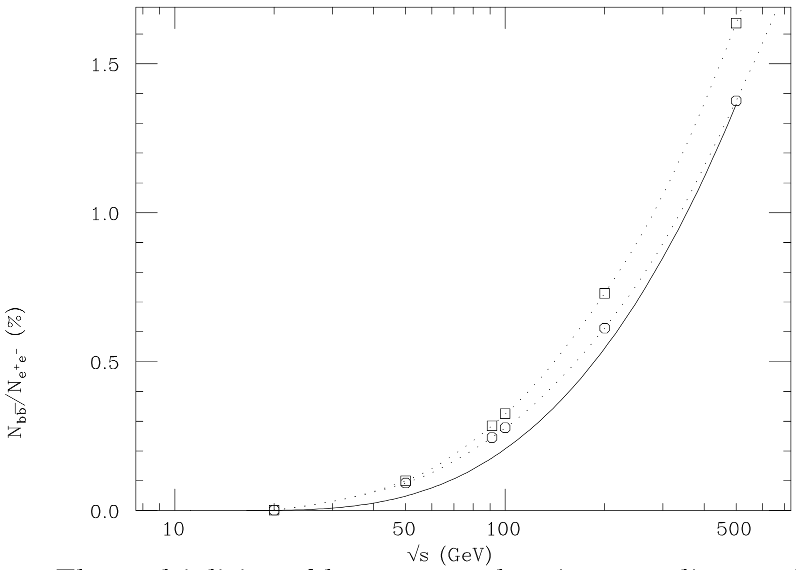

Figure 6: The multiplicity of bottom quark pairs according to the analytical result, using $\Lambda = 150$ MeV (solid). Points are from standard HERWIG (circles) and HERWIG modified to violate energy conservation (squares).

In order to do this, we have made a modified version of HERWIG that violates energy conservation in exactly the same way as next-to-leading order calculations. That is, when a quark emits a gluon, the gluon's energy is distributed correctly but the quark's energy remains unchanged. When a gluon emits another gluon, one of them has energy distributed according to the asymmetric gluon splitting function, $2(1-z)P_g^g(z)$, while the other keeps the full energy. This is achieved by first correctly generating both their energies, and then choosing one of them with probability in proportion to their energy to be the one that takes the full energy. For completeness, when a gluon splits to a quark-antiquark pair both are given the full energy, although this only gives rise to (next-to-)^{3}leading effects, and is numerically insignificant. Although the events thus generated are nonsensical, it does allow a direct estimate of the size of competition effects, since everything else is indeed equal. In Fig. 6 we show the results of doing this, where it can be seen that it makes a difference of about 15% for bottom quarks at the Z mass, rising slowly with energy (the ratio is reasonably fit by the form $\log\log\sqrt{s}$ over the whole $\sqrt{s}$ range we have considered, from 20 GeV to 10 TeV). For charm quarks it makes almost 25% difference.

In ARIADNE, multiple emission is always generated with strictly ordered transverse momentum, and this is also applied to gluon splitting[17]. This leads to an overcounting of final states, as can be seen from a formation-time argument[7], or by direct comparison with the matrix-element. We imagine the extreme case of a very heavy quark produced from a relatively low-$k_\perp$ gluon. In ARIADNE, this is possible provided the invariant p_t of the quark relative to its emitting dipole (which is roughly equivalent to the p_t relative to the gluon direction) is less than $k_\perp$. Thus the gluon splitting is very close to threshold, with the gluon virtuality equal to $2m_Q \gg k_\perp$. The formation-time of the emitted gluon, in its emitter's rest-frame is the virtuality of the emitting parton scaled by its Lorentz factor,

$$\tau_g \sim \frac{E}{Q}\,\frac{1}{Q} \sim \frac{1}{k_\perp \sin\theta}, \tag{28}$$

where θ is the opening angle between the gluon and the emitter. For a $\mathrm{Q\bar{Q}}$ pair of mass m, and the same $k_\perp$ and θ, the formation-time has two components, from the quark and gluon virtualities. If we assume that $k_\perp \ll m$, as is allowed in ARIADNE, then we obtain

$$\tau_{Q\bar{Q}} \sim \frac{E}{Q}\frac{1}{Q} + \frac{1}{m} \sim \frac{1}{\sqrt{k_\perp^2/\sin^2\theta + m^2} - k_\perp/\tan\theta} + \frac{1}{m} \sim \begin{cases} 1/m & \theta \sim \pi/2 \\ k_\perp/(m^2\theta) & \theta \ll 1 \end{cases}. \quad (29)$$

The condition of strongly-ordered formation times, $\tau_{Q\bar{Q}} \gg \tau_g$ is then

$$k_\perp \gg m \quad (30)$$

in both the small- and large-angle limits, contradicting our assumption, $k_\perp \ll m$. One only obtains a consistent formation-time picture, if strong ordering (30) is assumed. This limit depends only on the $Q\bar{Q}$ pair mass, and not on their kinematics, such as their invariant transverse momentum. It is strongly violated in ARIADNE, leading to an overestimate of the cross-section. Since the multiplicity of gluons increases rapidly with decreasing transverse momentum, this region of phase-space dominates the gluon-splitting process, so the overestimate is large. The usual prescription taken in Monte Carlo models is to replace the strong ordering conditions with strict ordering, requiring

$$k_\perp > m. \quad (31)$$

Another way to argue the same point is to consider the particle momenta after reconstruction of the recoils. Using a slightly simplified version of ARIADNE's recoil prescription, it is possible to exactly relate the $k_\perp$ and y originally generated for the gluon, to the variables we used in the leading order calculation (here relabeled $K_\perp$ and Y),

$$K_\perp^2 = k_\perp^2 + \left(1 - k_\perp/\sqrt{s}e^{-y}\right) m_g^2, \quad (32)$$

$$Y = y - \log\frac{K_\perp}{k_\perp}. \quad (33)$$

If we then assume that $k_\perp \ll \sqrt{s}$, we obtain

$$K_\perp^2 \approx k_\perp^2 + m_g^2, \quad (34)$$

and one finds that although gluons with arbitrarily small $k_\perp$ can contribute to gluon splitting of a given virtuality, they are all reconstructed with about the same value of $K_\perp^2$, corresponding to the same set of physical momenta, so this phase-space point is overcounted. In terms of cross-sections, this is

$$d\sigma \sim \frac{dk_\perp^2}{k_\perp^2} \sim \frac{dK_\perp^2}{K_\perp^2 - m_g^2}, \quad (35)$$

with an unphysical Jacobian peak at $K_\perp \sim m_g$. Recall that the matrix element contains $dK_\perp^2/K_\perp^2$, with phase-space limit $K_\perp > m_g$. Since $k_\perp \ll m_g$ is the region of large multiplicity, the overcounting is large.

We conclude that although it is well-known that $k_\perp$-ordering is appropriate for massless QCD, simply applying the same rules to processes with massive partons does not always work, and in the case of gluon splitting to massive quarks gives an overestimate of the cross-section. This could be corrected by applying an additional phase-space cut, requiring the virtuality of split gluons to be below the $k_\perp$ of their production. Results from a preliminary version of ARIADNE that includes this cut are considerably smaller, even falling below the parton shower models[18].

Another advantage of Monte Carlo models is that the mass of the original quarks can be easily incorporated, simply by modifying the $q \to qg$ splitting appropriately. On the other hand, the evolution equations that are solved to obtain the next-to-leading logarithmic multiplicities used above become much more complicated once quark masses are included. We have rerun the models with the correct admixture of quarks for e^+e^- annihilation, and find a suppression at the Z mass of about 10% from HERWIG and 5% from ARIADNE, both decreasing with increasing energy, and no significant suppression from JETSET. It is possible that this is due to different treatments of the 'dead cone' effect.

7 Summary

We have calculated the multiplicity of heavy quark pairs due to perturbative gluon splitting in e^+e^- annihilation to light quarks, accurate to leading order in α_s, and resumming large leading and next-to-leading logarithmic terms to all orders. At the Z mass, we obtain a bottom quark pair multiplicity of 0.18%, corresponding to 0.8% of the total bottom quark multiplicity. For charm quarks, the figures are 1.3% and 8% respectively.

Since our calculation neglects the effects of the original quark mass, we expect it to be an over-estimate by up to 10%. For bottom quarks we conservatively put the overall uncertainty at about 25%, and for charm quarks at about 30%. If our result and other multiplicity-type results in the next-to-leading logarithmic approximation are as correlated as expected, this uncertainty could be reduced by fits to the other data at the same energy.

Comparing our results with Monte Carlo models, we have found that those based on the parton shower approach agree reasonably well, while ARIADNE, based on the colour dipole model, does not. From our approximate expressions for the leading order matrix-element, we expected the CDM to be a better numerical approximation than DGLAP. The discrepancy appears to be caused by the use of the transverse momentum as the only ordering scale, even when the partons are massive. From our results using the modified version of HERWIG, we are confident that the large difference between ARIADNE and the parton shower models cannot be explained by competition effects.

Our results show that for bottom quarks, the gluon splitting process is becoming an important contribution to the measurement of the partial width of the Z boson to bottom quarks, at the accuracy to which current experiments are sensitive. For charm quarks it is already an essential component, and would even be expected to influence the shape of the energy spectrum, being dominantly at lower energy than direct charm quarks. Since the parton shower models predict the total multiplicity well, one would expect them to make at least a reasonable prediction of this energy spectrum.

Acknowledgments

I am grateful to Yuri Dokshitzer and Bryan Webber for many stimulating discussions of these and related topics. This work is supported in part by the EEC Programme "Human Capital and Mobility", Network "Physics at High Energy Colliders", contract CHRX-CT93-0537 (DG 12 COMA).

References

1. The ALEPH Collaboration, Phys. Lett. 244B (1990) 551,
   The DELPHI Collaboration, Phys. Lett. 252B (1990) 140,
   The OPAL Collaboration, Phys. Lett. 263B (1991) 311.
2. B.A. Schumm, Yu.L. Dokshitzer, V.A. Khoze, D.S. Koetke, Phys. Rev. Lett. 69 (1992) 3025.
3. The SLD Collaboration, Phys. Rev. Lett. 72 (1994) 3145.
4. A.H. Mueller, P. Nason, Phys. Lett. 157B (1985) 226; Nucl. Phys. B266 (1986) 265.
5. M.L. Mangano, P. Nason, Phys. Lett. 285B (1992) 160.
6. M.H. Seymour, Zeit. Phys. C63 (1994) 99.
7. Yu.L. Dokshitzer, V.A. Khoze, A.H. Mueller, S.I. Troyan, *Basics of Perturbative QCD*, Editions Frontières, Gif-sur-Yvette, 1991.
8. A.H. Hoang, M. Jeżabek, J.H. Kühn, T. Teuber, Phys. Lett. 325B (1994) 495, and erratum Phys. Lett. 327B (1994) 439.
9. The LEP Collaborations, CERN-PPE/93-157.
10. Yu.L. Dokshitzer, D.V. Shirkov, LU TP 93-19.
11. S. Catani, Yu.L. Dokshitzer, F. Fiorani, B.R. Webber, Nucl. Phys. B377 (1992) 445.
12. B.A. Kniehl, J.H. Kühn, Nucl. Phys. B329 (1990) 547.
13. G. Marchesini, B.R. Webber, G. Abbiendi, I.G. Knowles, M.H. Seymour, L. Stanco, Computer Phys. Comm. 67 (1992) 465.
14. M.Bengtsson, T.Sjöstrand, Phys. Lett. 185B (1987) 435; Nucl. Phys. B289 (1987) 810.
15. L. Lönnblad, Computer Phys. Comm. 71 (1992) 15.
16. Yu.L. Dokshitzer, Phys. Lett. 305B (1993) 295.
17. B. Andersson, G. Gustafson, L. Lönnblad, Nucl. Phys. B339 (1990) 393.
18. L. Lönnblad, private communication.

Table

$b\bar{b}$	Resummed + leading	0.177
	Leading order	0.100
	fCDM	0.101
	fDGLAP	0.120
	lCDM	0.128
	lDGLAP	0.150
	HERWIG, light quarks	0.246 ± 0.001
	JETSET, light quarks	0.163 ± 0.004
	ARIADNE, light quarks	0.342 ± 0.006
	HERWIG, all quarks	0.227 ± 0.001
	JETSET, all quarks	0.160 ± 0.004
	ARIADNE, all quarks	0.326 ± 0.006
	HERWIG, no E-conservation	0.285 ± 0.001
$c\bar{c}$	Resummed + leading	1.349
	Leading order	0.607
	HERWIG, light quarks	1.001 ± 0.006
	HERWIG, reduced m_c	1.523 ± 0.009
	JETSET, light quarks	1.764 ± 0.013
	JETSET, increased m_c	1.521 ± 0.012
	ARIADNE, light quarks	2.318 ± 0.015
	HERWIG, all quarks	0.923 ± 0.005
	JETSET, all quarks	1.701 ± 0.013
	ARIADNE, all quarks	2.177 ± 0.015
	HERWIG, no E-conservation	1.226 ± 0.007

Table 1: The multiplicity of heavy quark pairs at the Z mass in percent according to the various methods discussed in the text. The errors shown on the Monte Carlo results are purely statistical.

Appendix

In this appendix, we collect together details unnecessary for a casual reading of sections 2–4.

We integrate the curly bracket of (4) over the first two dimensions of (5),

$$
\begin{aligned}
&\int_{\log x_g}^{-\log x_g} dy \int_{x_g}^{(x_g^2+1)/2\cosh y} \frac{2dk_\perp}{k_\perp}\{\} && \text{(A1)}\\
&= 8(1+x_g^2)^2 \int_0^{-\log x_g} dy\; y\tanh y + 5 - 5x_g^4 + (6+8x_g^2+6x_g^4)\log x_g && \text{(A2)}\\
&= 4(1+x_g^2)^2 \left[\log^2 x_g - \int_{x_g^2}^1 dz \frac{-\log z}{1+z}\right] + 5 - 5x_g^4 + (6+8x_g^2+6x_g^4)\log x_g, && \text{(A3)}
\end{aligned}
$$

where the substitution $z = \exp -2y$ has been used. The remaining integral cannot be done analytically. The final integral is then

$$
\int_{x^2}^1 \frac{dx_g^2}{x_g^2}\sqrt{1-x^2/x_g^2}\left(1+\frac{x^2}{2x_g^2}\right)\{(\text{A3})\}\,. \qquad \text{(A4)}
$$

The remaining two-dimensional integration can be rewritten

$$
\begin{aligned}
&\int_{x^2}^1 \frac{dx_g^2}{x_g^2}\sqrt{1-x^2/x_g^2}\left(1+\frac{x^2}{2x_g^2}\right) 4(1+x_g^2)^2 \int_{x_g^2}^1 dz\frac{-\log z}{1+z} && \text{(A5)}\\
&= \int_{x^2}^1 dz \frac{-\log z}{1+z}\int_{x^2}^z \frac{dx_g^2}{x_g^2}\sqrt{1-x^2/x_g^2}\left(1+\frac{x^2}{2x_g^2}\right) 4(1+x_g^2)^2 && \text{(A6)}\\
&= \int_{x^2}^1 dz \frac{-\log z}{1+z}\left[\sqrt{1-\frac{x^2}{z}}\left(-\frac{20}{3} - 8x^2 - \frac{4x^2}{3z} + 8z + x^2 z + 2z^2\right)\right.\\
&\qquad \left. - (8-3x^4)\log x + (8-3x^4)\log\left(\sqrt{z}+\sqrt{z-x^2}\right)\right]. && \text{(A7)}
\end{aligned}
$$

Relabelling x_g^2 as z to give a single integration, we get the expression given in (6).

We next integrate the first term of the curly bracket of (4) over the first two dimensions of (10),

$$
\begin{aligned}
&\int_{-\cosh^{-1}1/2x_g}^{\cosh^{-1}1/2x_g} dy \int_{x_g}^{1/2\cosh y} \frac{2dk_\perp}{k_\perp}\{\} && \text{(A8)}\\
&= 8\int_0^{\cosh^{-1}1/2x_g} dy\; y\tanh y + 6\sqrt{1-4x_g^2} + 6\log x_g - 6\log\left(\tfrac{1}{2}+\tfrac{1}{2}\sqrt{1-4x_g^2}\right)\\
&= 4\left[\log^2 x_g - \log^2 2 + \int_{x_g^2}^{1/4}\frac{dz}{z}\log\left(\tfrac{1}{2}+\tfrac{1}{2}\sqrt{1-4z}\right)\right] && \text{(A9)}\\
&\quad +6\sqrt{1-4x_g^2} + 6\log x_g - 6\log\left(\tfrac{1}{2}+\tfrac{1}{2}\sqrt{1-4x_g^2}\right).
\end{aligned}
$$

The two-dimensional integral can be transformed to a one-dimensional one in exactly the same way, so we obtain

$$\mathcal{N}_{\mathrm{fCDM}} = \left(\frac{\alpha_s}{4\pi}\right)^2 \frac{4}{3} C_F \int_{x^2}^{1/4} dz \Bigg\{$$

$$\frac{1}{z}\sqrt{1-\frac{x^2}{z}}\left(1+\frac{x^2}{2z}\right)\Bigg[\log^2 z - \log^2 4 + 6\sqrt{1-4z}$$

$$+ 3\log z - 6\log\left(\tfrac{1}{2}+\tfrac{1}{2}\sqrt{1-4z}\right)\Bigg]$$

$$+\frac{\log\left(\frac{1}{2}+\frac{1}{2}\sqrt{1-4z}\right)}{z}\Bigg[\sqrt{1-\frac{x^2}{z}}\left(-\frac{20}{3}-\frac{4x^2}{3z}\right)$$

$$- 8\log x + 8\log\left(\sqrt{z}+\sqrt{z-x^2}\right)\Bigg]\Bigg\}. \tag{A10}$$

The modification of (12) corresponds to

$$2 - 4k_\perp \cosh y + 2k_\perp^2 \cosh 2y \longmapsto 2 - 4k_\perp \cosh y + 2k_\perp^2(\cosh 2y + 1). \tag{A11}$$

Following the same steps, we obtain,

$$\mathcal{N}_{\mathrm{fDGLAP}} = \left(\frac{\alpha_s}{4\pi}\right)^2 \frac{4}{3} C_F \int_{x^2}^{1/4} dz \Bigg\{$$

$$\frac{1}{z}\sqrt{1-\frac{x^2}{z}}\left(1+\frac{x^2}{2z}\right)\Bigg[\log^2 z - \log^2 4 + 7\sqrt{1-4z}$$

$$+ (3+2z)\log z - (6+4z)\log\left(\tfrac{1}{2}+\tfrac{1}{2}\sqrt{1-4z}\right)\Bigg]$$

$$+\frac{\log\left(\frac{1}{2}+\frac{1}{2}\sqrt{1-4z}\right)}{z}\Bigg[\sqrt{1-\frac{x^2}{z}}\left(-\frac{20}{3}-\frac{4x^2}{3z}\right)$$

$$- 8\log x + 8\log\left(\sqrt{z}+\sqrt{z-x^2}\right)\Bigg]\Bigg\}. \tag{A12}$$

The leading approximations are slightly simpler, but follow the same steps to give,

$$\mathcal{N}_{\mathrm{lCDM}} = \left(\frac{\alpha_s}{4\pi}\right)^2 \frac{4}{3} C_F \int_{x^2}^{1/4} dz \Bigg\{$$

$$\frac{1}{z}\left[\log^2 z - \log^2 4 + 6\sqrt{1-4z} + 3\log z - 6\log\left(\tfrac{1}{2}+\tfrac{1}{2}\sqrt{1-4z}\right)\right]$$

$$-4\frac{\log\left(\frac{1}{2}+\frac{1}{2}\sqrt{1-4z}\right)}{z}\log\frac{x^2}{z}\Bigg\}. \tag{A13}$$

$$\mathcal{N}_{\mathrm{lDGLAP}} = \left(\frac{\alpha_s}{4\pi}\right)^2 \frac{4}{3} C_F \int_{x^2}^{1/4} dz \Bigg\{$$

$$\frac{1}{z}\left[\log^2 z - \log^2 4 + 7\sqrt{1-4z} + (3+2z)\log z - (6+4z)\log\left(\tfrac{1}{2}+\tfrac{1}{2}\sqrt{1-4z}\right)\right]$$

$$-4\frac{\log\left(\frac{1}{2}+\frac{1}{2}\sqrt{1-4z}\right)}{z}\log\frac{x^2}{z}\Bigg\}. \tag{A14}$$

To obtain (18), we need to calculate the integral

$$I = \int_{z_0}^{z_1} \frac{dz}{z} \mathcal{N}^+(z, z_1), \tag{A15}$$

keeping track of next-to-leading order corrections. Making repeated use of the relations

$$\begin{aligned}
\int dz z^\nu K_{\nu+1}(z) &= -z^\nu K_\nu(z) + 2\nu \int dz z^{\nu-1} K_\nu(z), &\text{(A16)}\\
\int dz z^\nu I_{\nu+1}(z) &= z^\nu I_\nu(z) - 2\nu \int dz z^{\nu-1} I_\nu(z), &\text{(A17)}
\end{aligned}$$

we obtain to next-to-leading order,

$$\begin{aligned}
I = &\left[\frac{1}{z_1^{B-1}} \left\{-z^{B-1} I_{B+1}(z_1) K_{B-1}(z) - 2(B-1) z^{B-2} I_{B+1}(z_1) K_{B-2}(z)\right.\right.\\
&\left.\left. + z^{B-1} K_{B+1}(z_1) I_{B-1}(z) - 2(B-1) z^{B-2} K_{B+1}(z_1) I_{B-2}(z)\right\}\right]_{z_0}^{z_1}. \qquad \text{(A18)}
\end{aligned}$$

Using the relations

$$\begin{aligned}
I_{\nu+1}(z) &= I_{\nu-1}(z) - \frac{2\nu}{z} I_\nu(z), &\text{(A19)}\\
K_{\nu+1}(z) &= K_{\nu-1}(z) + \frac{2\nu}{z} K_\nu(z), &\text{(A20)}
\end{aligned}$$

we obtain

$$\begin{aligned}
I = &\left[\frac{1}{z_1^{B-1}} \left\{-z^{B-1} I_{B-1}(z_1) K_{B-1}(z)\right.\right.\\
&+ 2B z^{B-1}/z_1 \, I_B(z_1) K_{B-1}(z) - 2(B-1) z^{B-2} I_{B+1}(z_1) K_{B-2}(z)\\
&+ z^{B-1} K_{B-1}(z_1) I_{B-1}(z)\\
&\left.\left. + 2B z^{B-1}/z_1 \, K_B(z_1) I_{B-1}(z) - 2(B-1) z^{B-2} K_{B+1}(z_1) I_{B-2}(z)\right\}\right]_{z_0}^{z_1}. \qquad \text{(A21)}
\end{aligned}$$

Finally, since the second and fourth lines are next-to-leading we can shift the indices of the Bessel functions to any convenient values, so we obtain (18). Similar steps give (20).